

# Geophysical Research Letters®



## RESEARCH LETTER

10.1029/2021GL095601

### Key Points:

- Measurements of 337- and 777-nm irradiances in long-gap discharges are acquired simultaneously with current and short-time exposure images
- Blue optical emissions (337 nm) are associated with streamer development and negative leader stepping
- During stable leader propagation, red optical emissions (777 nm) are predominant over the blue

### Supporting Information:

Supporting Information may be found in the online version of this article.

### Correspondence to:

M. Arcanjo,  
[marcelo.augusto.sousa@upc.edu](mailto:marcelo.augusto.sousa@upc.edu)

### Citation:

Arcanjo, M., Montanyà, J., Urbani, M., & Lorenzo, V. (2021). Optical signatures associated with streamers and leaders of laboratory discharges. *Geophysical Research Letters*, 48, e2021GL095601. <https://doi.org/10.1029/2021GL095601>

Received 6 AUG 2021

Accepted 8 OCT 2021

## Optical Signatures Associated With Streamers and Leaders of Laboratory Discharges

M. Arcanjo<sup>1,2</sup> , J. Montanyà<sup>1</sup> , M. Urbani<sup>1</sup> , and V. Lorenzo<sup>2</sup> 

<sup>1</sup>Electrical Engineering Department, Polytechnic University of Catalonia, Barcelona, Spain, <sup>2</sup>Dena Desarrollos S. L. (Ingesco), Terrassa, Spain

**Abstract** This work investigates the strongest optical emissions associated with long laboratory sparks (at the wavelengths of 337 and 777 nm) with the aim to understand similar emissions in lightning. The processes of the long-spark formation are studied by using optical measurements, current signatures, and short-time exposure images. Blue optical emissions (337 nm) are associated with streamer development and negative leader stepping, and the optical pulses have good correlation with current pulses. Red optical emissions (777 nm) are mainly associated with stable leader propagation, when this irradiance is predominant over the blue one. The results indicate that formations of stems from positive leaders also produce emissions at 777 nm. This work aims to support satellite-based measurements that perform optical measurements in the same wavelength ranges.

**Plain Language Summary** Lightning is a fast discharge characterized by the propagation of current waves through plasma channels. These surge events produce optical emissions all over the spectra (from ultraviolet to infrared) associated with physical processes of the main components of the lower atmosphere (Nitrogen and Oxygen) and their interaction with the lightning channel. The study of optical signatures from thunderstorms performed in satellites has contributed to a better understanding of processes related to lightning. In this work, we investigate the strongest optical emissions associated with long laboratory sparks (at the wavelengths of 337 and 777 nm). Altogether with current signatures and short-time exposure images, we characterized the processes that produce these emissions to support satellite-based measurements.

## 1. Introduction

The advent of new technologies and the improvement of sensors embedded in satellites have allowed optical observations of diverse phenomena associated with lightning. Measurements of radiances from the cloud top consider all types of lightning during day and night, mainly based on the emissions of the oxygen triplet band at 777.4 nm (e.g., Chern et al., 2003; Christian et al., 1989; Goodman et al., 2013; Kirkland et al., 2001; Neubert et al., 2019). The use of satellite-based instruments, combined with other mapping techniques, provides comprehensive details for lightning investigation. The information obtained by satellites requires careful analysis due to the complexity of lightning-associated phenomena: processes before the return stroke such as the propagation of streamers and leaders inside the clouds, impulsive currents that usually last microseconds during the return strokes, recoil leaders, long continuous currents that can last milliseconds, and subsequent events correlated such as blue jets, sprites, and elves (Neubert et al., 2008; Rakov & Uman, 2003). Surges in 777.4-nm luminosity were associated with return stroke currents, recoil leaders, and leader branching processes (Montanyà et al., 2021; van der Velde et al., 2020).

In 2018, the Atmosphere-Space Interactions Monitor (ASIM) was launched to obtain information from Transient Luminous Events (TLE) and terrestrial gamma-ray flashes (TGFs) caused by the activity of thunderstorms. It is equipped with three high-speed photometers at 180–230, 337, and 777.4 nm, with sampling rates up to 100 kHz (Chanrion et al., 2019). Recently, Li et al. (2021) and Soler et al. (2020) reported blue flashes associated with narrow bipolar events (NBEs) with no simultaneous activity at 777.4 nm; Neubert et al. (2021) showed detections from a blue jet into the stratosphere with emissions in the ultraviolet range and faint and localized emissions in the red spectral band. These studies suggest that the blue flashes and the jet are associated with non-thermal processes of cloud corona and streamer ionization waves.

© 2021 The Authors.

This is an open access article under the terms of the [Creative Commons Attribution-NonCommercial](https://creativecommons.org/licenses/by-nc/4.0/) License, which permits use, distribution and reproduction in any medium, provided the original work is properly cited and is not used for commercial purposes.

Laboratory techniques have allowed a better understanding of optical emissions occurring during lightning. A broad review on lightning spectroscopy and the high-speed spectra of meter-long laboratory discharges in a wide range (between 380 and 800 nm) were recently explored by Kieu et al. (2021). During the breakdown, they have found several optical emissions similar to those found in natural lightning. Gallimberti et al. (1974) and Les Renardières (1981) showed the similarities between the near UV spectra of first coronas and leader coronas. The spectra are composed mainly by the radiation of the nitrogen second positive system. High-speed photography and imaging systems have also been making progress and revealing details of the formation and propagation of discharges. ICCD cameras have been used for obtaining streak images, taking short-exposure pictures, or full stroboscopic images that can assess rapid streamers' formation (e.g., Bazelyan et al., 2007; Kochkin et al., 2014; Kochkin et al., 2016; Nijdam et al., 2020). Schlieren images use the observation of changes in temperature (i.e., gas density) to distinguish stem channels from streamer filaments that cause a minimal air density change (e.g., Zhao, Becerra, et al., 2021; Zhao, Liu, et al., 2021).

Janda and Macha (2011) and Janda et al. (2012, 2016) conducted several experiments with transient sparks in very short gaps (mm range) for investigating the optical emission spectra associated to streamer-to-spark transition and NO<sub>x</sub> generation. The discharges were imaged with fast ICCD cameras and characterized with a spectrometer and photometers with narrowband filters centered in the 337 and 777 nm. The streamer development produces strong emissions in the nitrogen second positive system, while the spark phase exhibits strong atomic emissions (such as the oxygen triplet at 777 nm). By increasing the frequency of the discharges, they were able to decrease the intensity of the atomic emissions. They found that the streamer-to-spark transition is governed by the increase in the gas temperature in the plasma channel up to about 1000 K. This stage also presents the emergence of the 777-nm emissions, indicating the production of O species.

To provide a better understanding of satellite-based optical measurements of lightning discharges, this work investigates optical signatures of long-air gap (0.85–1 m) discharges produced with a Marx Generator.

## 2. Methodology

The high voltage experiments were carried out at LABELEEC, in Terrassa (Spain). We present unprecedented optical signatures of the aforementioned spectral ranges (near 337 and 777 nm) correlated with the applied voltage and ground current during the streamer and leader phases. Additionally, we image the discharges at the moment of strong emissions obtained by the photometers with short-time exposure pictures. The optical emissions associated with the discharges within the response range of our filters can be attributed mainly to the radiation of the second positive system of nitrogen molecules (Gallimberti et al., 1974) in the blue (337 nm) and to the radiation of the neutral O I line in the red (777 nm), which is in reality a triplet with sublines at 777.19, 777.42, and 777.54 nm (Kieu et al., 2021).

To investigate the streamer and leader inception and their signatures, we employed two different setups. In the first configuration (plate-to-rod), the high voltage was connected to a hanging plate with 2 m of diameter standing 2 m above the floor. The ground electrode stood one meter high, leading to a gap distance of 1 m. We provided an alternative discharge path, which consisted of a sphere-to-sphere configuration, separated by approximately 30 cm. That allows streamers and leaders to develop from the ground electrode in the main gap, but the breakdown can occur in either gap. In the second configuration, there is only one discharge path with a rod-to-rod arrangement and a gap distance of 0.85 m. In both cases, the photomultipliers (PMTs) are located 2.7 m away from the ground electrode and have a wide field of view of the gap. We provide a detailed description of the instrumentation and methods in Supporting Information S1.

## 3. Positive Leaders

When a positive voltage is applied to an electrode providing a certain level of electric field enhancement, avalanche activities in the proximity of the rod may lead to the formation of streamers, namely first coronas. One or more dark periods may follow, and secondary streamer corona bursts can trigger the formation of a thermalized gas channel forming the stem. The corona stem structure is heated up to a threshold level (1,200–2000 K) that enables the leader development (Gallimberti et al., 2002; Jiang et al., 2020).

Once established, a brush-like corona zone with positive streamers directs the leader propagation (Rakov & Uman, 2003; Saba et al., 2020).

In our experiments, we used the plate-to-rod setup, applying negative voltage at the upper plate. Since the local electric field thresholds needed for sustained propagation of positive leaders is much lower than for negative leaders (Bazelyan & Raizer, 2000), we measured currents and optical signatures solely due to the positive streamer/leader propagation from the grounded rod toward the plate.

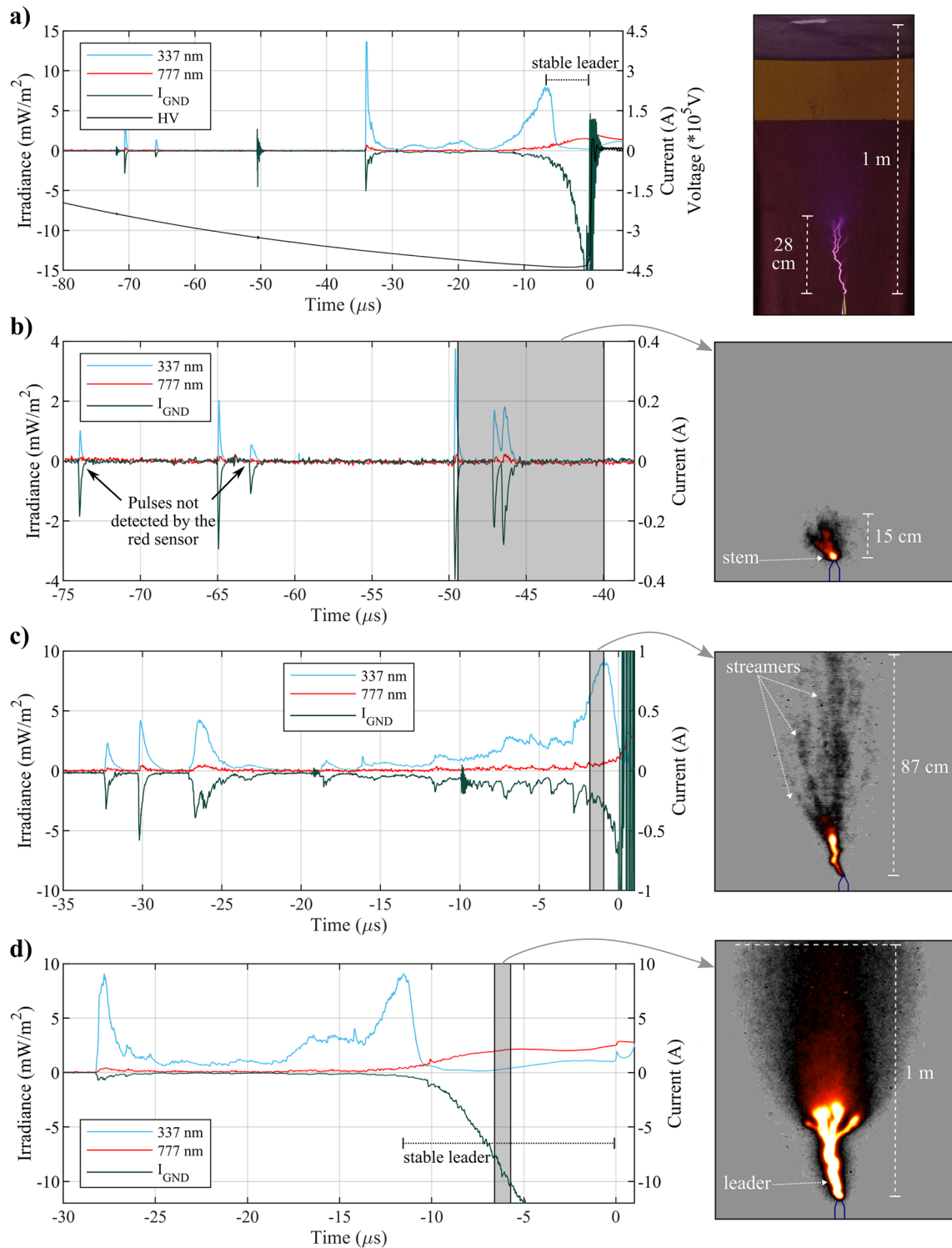
In Figure 1, we show signals measured for four positive discharges with corresponding pictures displayed on the right side. A color coding scheme is applied to the original picture to enhance faint streamers (Kochkin et al., 2014). The time scales presented consider the breakdown occurring at  $t = 0$  s. Figure 1a shows the last 80  $\mu\text{s}$  of an aborted leader formation. The voltage increases up to 440 kV, and a few current pulses are recorded. At  $t = -35 \mu\text{s}$ , a pulse of 1.5 A produces optical emissions detected by both PMTs. The current decays in about 2  $\mu\text{s}$  but a small quasi-DC component of tens of milliamperes is measured. The blue pulses indicate streamers developing in the main gap. At  $t = -15 \mu\text{s}$ , the blue irradiance increases smoothly, as well as the current, and the red irradiance starts to increase later, at  $t = -10 \mu\text{s}$ . The blue signal reaches another peak at  $t = -6.5 \mu\text{s}$  and, after that, reduces intensity substantially. From this moment on, the increase in the current accelerates along with the red signal, characterizing a stable leader development from the ground electrode. When the breakdown occurs (at the spheres adjacent to the main gap) the voltage at the upper plate collapses to zero and the leader development is aborted. The charges stored in the forming leader are rapidly induced back to the electrode. This process is characterized by oscillations in the current and an impulse in the red signal. On the right side of Figure 1a, the still picture shows the upward leader that propagated over a vertical distance of 28 cm.

Figure 1b depicts pulses from the initial stage of the discharge when the upper plate voltage was in the range of 300–350 kV (negative). The irradiance in the blue is similar to the current, while the irradiance in the red exhibits mild pulses. Using the ICCD camera, an image with a time exposure of 9.5  $\mu\text{s}$  was captured, showing the formation of a stem around the tip of the electrode and a burst of short (15 cm) streamers that emerges from the stem. In the early stage of the voltage rise, several current pulses of low amplitudes did not produce detectable pulses in the red. Our results indicate that red pulses such as shown in Figure 1b might be related to the presence of stems and thermal processes associated to the streamer-to-leader transition.

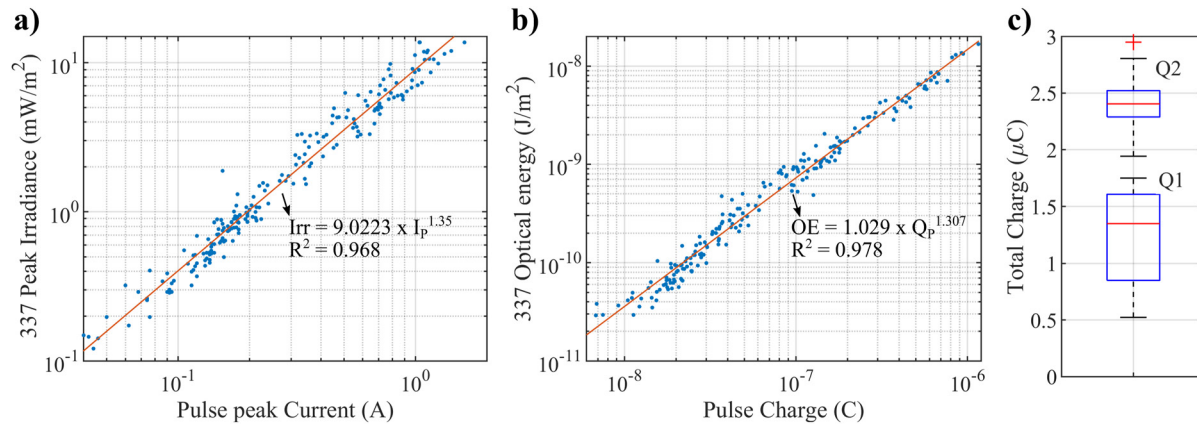
The initial stage of the leader development is shown in Figure 1c in which an image with a time-exposure of 0.9  $\mu\text{s}$  was taken just before the peak of the blue irradiance. The leader has a vertical length of roughly 15 cm, and one can see that streamers from the leader's tip propagate quite far across the gap, close to reaching the upper plate (about 72 cm). In the remaining microsecond before the breakdown, the current and the intensity of the red continues to increase. On the contrary, the blue irradiance decreases.

Figure 1d shows the later stage of a stable leader propagating upwards with the corresponding image (0.9  $\mu\text{s}$  time-exposure) taken 3.5  $\mu\text{s}$  after the peak of the blue signal. At this point, the red optical emissions completely overcome the blue emissions. Ahead of the leader, one can note a cloud of light immersed in the gap resembling a conical volume. This is part of the corona region in front of the leader and can also be seen in Figure 1a as a purple blur in front of the streamers' tip. In the last 5  $\mu\text{s}$  depicted by Figure 1d, the blue irradiance increases slightly until the breakdown. The peak of the blue signal at the breakdown is much less intense than the peak observed during the streamer burst in the initial stage of the leader. The peak of the red irradiance occurs at the breakdown and saturates the photosensor.

We investigated the correlation between the optical irradiances and the current of a single streamer burst. The time duration of each burst varies between 600 ns and 7  $\mu\text{s}$ . In Figure 2a, we show a logarithmic scattered plot of the pulse peak current and the blue peak irradiance. We found a good relationship that can be best fitted to a power-law function, as indicated in the figure. The largest peak current observed during this regime was 1.2 A. We also calculated the individual charge of each burst, considering the same time segments correlated with the received optical energies by integrating the irradiance measured by the PMT. The results presented in Figure 2b confirm similar agreement between the variables. Comparable findings were reported by Janda et al. (2016) for the streamer stage in short gap transient discharges.



**Figure 1.** Irradiance (blue and red) and current (green) measured for four different discharges. In (a)–(c), the breakdown takes place in the sphere-to-sphere setup whereas in (d), it occurs in the main gap. (a) Upper plate negative voltage increase, PMTs measurements over 80  $\mu s$  and 3-s still picture of the development of the aborted upward leader. (b) Pulses of current and irradiances during the formation of a stem with surrounding streamers in a 9.5- $\mu s$  picture. (c) Streamer burst at the peak of the blue irradiance. The forming leader is observed in a 0.9- $\mu s$  picture. (d) Optical signals and current signals during the stable leader development toward the upper plate.



**Figure 2.** Optical irradiance and energy are associated with pulse peak current and pulse charge of positive discharges from the ground electrode. (a) For pulse peak current ranges from 40 mA to 1.6 A, the peak irradiance is shown for the blue photosensor. (b) The optical energy of each burst with the corresponding charge. (c) Total charge obtained during the voltage rise for two grouped discharges: Q1 when there is no evident blue collapse for increasing current and Q2 otherwise.

The same analysis was performed for the signals recorded in the red. These results are shown in Figure S3 in Supporting Information S1 for the sake of completeness. Compared to the blue, the red radiation does not present a good correlation with the current and charge. Initial streamer bursts that start to heat up the forming plasma channels during the voltage rise did not produce detectable optical pulses in the red.

We grouped the discharges performed with the plate-to-rod setup, classifying them if the stable leader development was detected or not. As indicated in Figures 1a and 1d, this is characterized by the collapse in the blue signal, followed by increasing currents and stronger emissions in the red. All discharges were performed with  $-650$  kV set at the Marx Generator. Figure 2c shows a boxplot with the total charge associated with the discharges of the two groups. For the discharges that did not present the stable leader development (Q1), the total charge is computed from the start of the voltage rise until the breakdown. For the second group (Q2), the charge is calculated until the peak of the blue irradiance is reached. The two groups presented a clear separation between the charge values observed. The obtained averages were  $1.3 \mu\text{C}$  for Q1 and  $2.4 \mu\text{C}$  for Q2. We determined the average ground current at the moment of the peak in the blue for the discharges of Q2, corresponding to  $388$  mA and standard deviation of  $98$  mA (excluding one outlier value of  $1.9$  A).

By using the images obtained with short and long time-exposure for the discharges, the results indicate that the blue peak irradiance is associated with the streamer burst all over the gap, which is a precursor for the stable leader development. Note that our group criterium is different than the concept of streamer-to-leader transition. The minimum amount of charge for a single or successive corona burst required for the thermal transition is estimated in the range of  $0.2$ – $1.0 \mu\text{C}$  (e.g., Arevalo & Cooray, 2017; Gallimberti, 1979; Wu et al., 2013). From our analysis, stems and leaders are incepted prior to the peak of blue irradiance, such as the cases shown in Figures 1b and 1c. The individual burst charges in those cases are within the range previously reported. Nevertheless, the group criterium introduced here presents a good agreement with the red irradiance and the current acceleration, features of the sustained leader development.

### 3.1. Effect of Multiple Tips at the Ground Electrode

We explored the effect of multiple tips at the ground electrode on optical emissions and currents. The single sharp tip coupled to the ground electrode was changed for a multiple-tip electrode coupled to a rectangular metallic plate and five tips in total (see Figure S4 in Supporting Information S1).

For this experiment, we compared the streamers formed at the two ground electrodes by triggering the camera at the same upper plate voltage levels. The image acquisition was performed with time-exposures of  $10 \mu\text{s}$  (see Figure S4 in Supporting Information S1). Discharges with the single tip present fewer pulses, but with greater amplitude (in both current and blue sensor), whereas the discharges produced by multiple tips

present more pulses, although weaker. We observe that even very small current pulses (less than 100 mA) emit in the blue range. The irradiance in the red also presents some correspondence with the current pulses, as previously discussed. From the images, we also saw bright spots from the electrodes' tips, which could be an indication of forming stems.

Noteworthy, we have performed discharges using a rod-to-rod setup with a positive voltage applied on the upper electrode. The electric field enhancement provided by this configuration favors the initiation of positive streamers/leaders (Bazelyan & Raizer, 2000), as it can be seen from the measurements of irradiances in the blue (see Figure S5 in Supporting Information S1 for typical waveforms and images). The mechanism of stable leader acceleration (denoted by the increase of red irradiance and decrease of blue irradiance) is the same as discussed for the plate-to-rod setup.

#### 4. Negative Leaders

In the laboratory, when a negative voltage is applied to an electrode, the consequent increase in the local electric field provided by the electrode tip can lead to the inception of negative streamers. At a reduced distance from the front of the streamers, a small plasma structure (space stem) can form. Bidirectional streamers originate from this plasma body, according to the local electric field. In the posterior region of the stem, positive streamers are formed, while negative streamers are established at the other end. Upon reaching higher temperatures, the stem evolves into a floating plasma channel (space leader). The propagation of the main negative channel consolidates after the attachment of the positive portion of the floating leader to the negative electrode streamers. This process leads to an abrupt extension of the length of the channel (step). Following the transfer of potential from the electrode to the end of the newly incorporated floating channel, new negative streamers are formed, and the process repeats, continuing the negative leader propagation (Bazelyan & Raizer, 2000; Biagi et al., 2010; Gallimberti et al., 2002; Rakov & Uman, 2003).

For these experiments, we used the rod-to-rod setup with a gap of 85 centimeters. It is crucial to acknowledge that the optical signals presented here correspond to discharge developments from both electrodes. Furthermore, the ground current is disturbed by discharges at the high voltage electrode due to capacitive coupling.

Figure 3 shows irradiances and the ground current for negative discharges in switching impulse. The voltage at the upper rod increases up to around 600 kV, and a small number of current pulses are observed. The blue irradiance presented some pulses of low amplitude during the voltage rise, likely related to the negative streamers that are incepted from the upper rod. Negative coronas in the air usually have less current amplitude and are fainter than positive coronas for similar high voltage levels (Arcanjo et al., 2020). We did not observe evident pulses of red irradiance before the last 5  $\mu$ s of the discharges. Although the charging voltage of the Marx Generator is higher in this case, the rod-to-rod configuration with a negative voltage applied does not favor positive stem/leader inception from the ground electrode, as it occurs for the plate-to-rod setup (see Figure 1).

Figure 3a depicts an interval of 20  $\mu$ s before the breakdown. At  $t = -4 \mu$ s, a strong pulse is measured by the photometers and the current sensor. This pulse reaches a blue peak irradiance of 38 mW/m<sup>2</sup> and a peak current (measured at the ground electrode) of 0.85 A. A 5- $\mu$ s time-exposure image is taken during the moment indicated by the shaded region shown in Figure 3a, revealing a glowing sphere-like volume around the high voltage electrode. This structure is connected to a secondary volume that is located at about 11.8 cm below the electrode tip, indicating a space stem formation, similar to the ones reported by Les Renardieres (1981), Reess et al. (1995), and Kochkin et al. (2014). From the ground electrode, a dim streamer-like shape can be noticed. A second pulse at  $t = -2.9 \mu$ s, completes the single-step process before the stable leader propagation. The blue peak irradiance is 24 mW/m<sup>2</sup> and, after the pulse, the current increases sharply, followed by the collapse of the blue signal and the increase in the red signal until the moment of the breakdown (at  $t = 0$ ).

Figure 3b shows data from another discharge, in which only one large pulse in the blue is observed before the stable leader development. On the right side of the figure, an image taken with time-exposure of 80 ns reveals leaders propagating from both electrodes. At this moment, the current at the ground electrode is 45

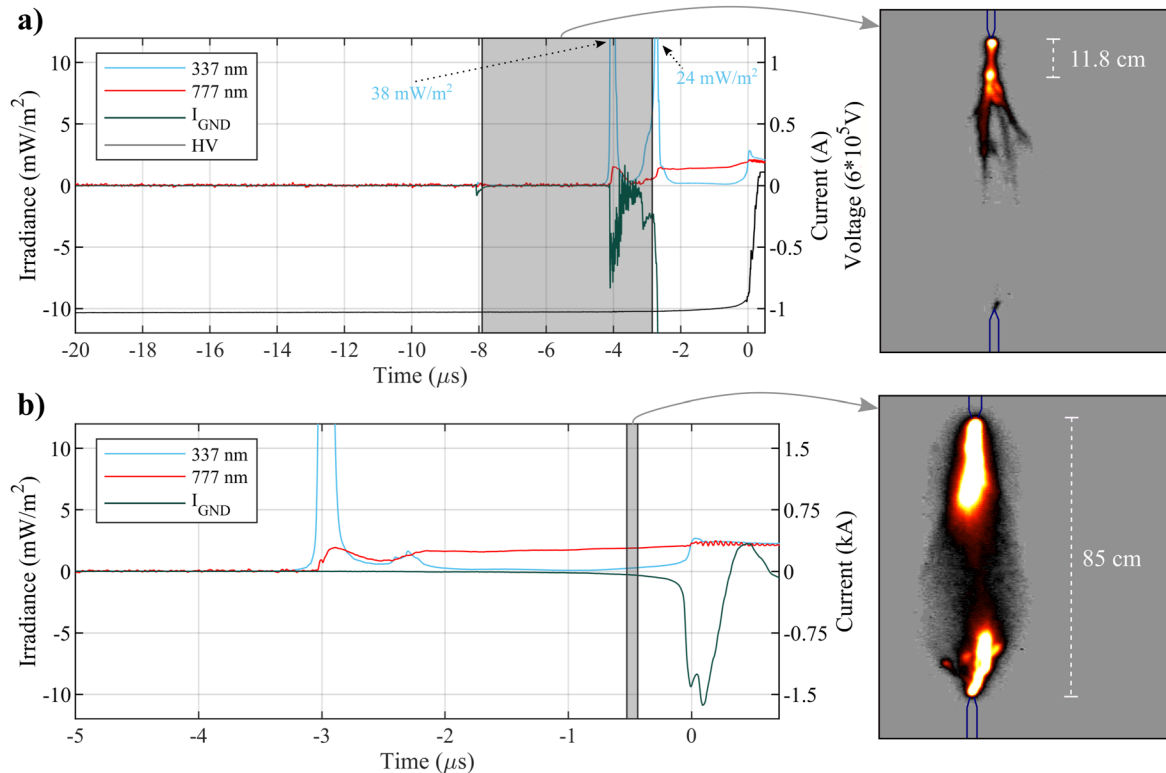


**Figure 3.** Optical emissions and current during the final stage of two negative rod-to-rod discharges. (a) The 4.5- $\mu$ s time-exposure image shows features of stepping of the negative leader and a space stem formed 11.8 cm below the electrode tip. (b) The leader stage consolidation with stronger red emissions. The negative and positive leader developments are shown in an 80-ns image taken 500 ns before the discharge.

A. Although the leaders saturate the image, it is possible to appreciate positive leader branches propagating behind the connecting channel. They are “connected” to the negative leader tip by a glowing zone, similar to the positive upward leader shown in Figure 1d.

For both discharges shown in Figure 3, during the last two microseconds before the breakdown, the red irradiance slowly increases as well as the blue irradiance, although in different levels. The peak irradiances align with the first current peak of about 1.4 kA, but the red signal saturates. After that, the current waveform reaches its peak (roughly 1.6 kA) and decays rapidly, oscillating in both polarities before returning to zero. The blue irradiance observed during the discharge current is drastically lower than the pulses observed during the stepping process.

## 5. Discussion and Implications for Lightning

We observed that the positive leader development is characterized by the increase of the emissions at the 777-nm wavelength. Nevertheless, weaker current pulses during the voltage rise, also produced such emissions when stems are incepted (see Figure 1). That is expected to be related to the thermalization process during the positive streamer-to-leader transition. For initial current pulses measured during the voltage rise, we did not observe 777 emissions, similarly to Janda et al. (2016), who performed transient discharges in a particular setup. Zhao, Liu, et al. (2021) showed millimeter-long stems since the first streamer burst, and that later streamer bursts could branch and elongate stems, driving the propagation of positive leaders. Their findings provide valuable contributions to the role of stems heating the precursor leader path. In our experiments, the major emissions in the red starts during the stable leader development (after the streamer burst marked by a peak and collapse of the blue emissions). The red irradiance increases along with the uprising continuous current and a slight increase in the blue irradiance (see Figure 1d) before breakdown.

Blue optical emissions are associated with streamer development, and negative leader stepping, and are expected to be observed in satellite-based observations of activities that involve positive and negative leader propagation. We have found a significant correlation between the peak emissions at the 337-nm wavelength and the peak current of burst streamer pulses (see Figure 2a). Janda et al. (2016) found a similar agreement comparing the waveforms of detections at 337 nm with the streamer current. We also noted an improved correlation between the optical energy and the pulse charge (see Figure 2b). The use of multiple tips for the ground electrode increases the number of current pulses observed during the voltage rise. The correlation between the current and the blue irradiance persists, yet both present significantly lower amplitudes.

The stable leader propagation takes place with the remarkable increase and acceleration of the current and the red irradiance. That happens after the peak and collapse of the blue irradiance. By grouping the discharges whether they presented the stable leader development, we calculated the total charge “dissipated” from the beginning of the voltage rise. The average total charges found were significantly different: 1.3  $\mu\text{C}$  for the first group (Q1) and 2.4  $\mu\text{C}$  for Q2, calculated up to the moment when the stable leader is detected (see Figure 2c).

We measured blue emissions associated with negative streamers during the voltage rise in the rod-to-rod experiment. They are more difficult to see due to their lower amplitude and shape (Arcanjo et al., 2020). We observed a large pulse in the blue associated with the negative leader inception and step (see Figure 3a). This pulse presents irradiances considerably higher than for the positive leader. We have left for future works a closer-look temporal analysis of emissions during the breakdown, since for now, our PMT saturated.

The development of in-cloud positive leaders with corona brushes leading its propagation is expected to produce emissions content in both blue and red regions. The same should be expected in the stepped fashion propagation of negative leaders, with streamers guiding the connection between the leader tip and the space stems/leaders. That is consistent with similar 337 and 777 nm signatures for several events observed by the ASIM mission (e.g., Heumesser et al., 2021; Neubert et al., 2019; Østgaard et al., 2019).

Blue flashes and other events with an absence of emissions in the red are associated with cold discharges characterized by traveling streamers inside the clouds such as in NBEs (Cooray et al., 2020; Li et al., 2021; Soler et al., 2020). The high currents associated with these events (estimated in the order of tens of kiloamperes) produce narrow but strong irradiating signals (Rison et al., 2016). Using the relationship provided in Figure 2a between peak current and peak irradiance measured in our setup, we extrapolated the irradiance for peak currents such as the ones of fast breakdown. For a peak current value of 55 kA, we estimated irradiances measured at ASIM’s distance (400 km) with values of roughly 1  $\mu\text{W}/\text{m}^2$  (see Supporting Information S1 for details). This value is within the order of magnitude of those measured by ASIM, about 10  $\mu\text{W}/\text{m}^2$  (Soler et al., 2020). In future works we intend to deepen the calculations of such quantities, considering more events reported by ASIM and atmospheric effects that can interfere on the calculations.

## Data Availability Statement

Measurements and data file supporting the conclusions are available at: <https://doi.org/10.7910/DVN/IPC94J>.

## References

- Arcanjo, M., Montanyà, J., Urbani, M., Lorenzo, V., & Pineda, N. (2020). Observations of corona point discharges from grounded rods under thunderstorms. *Atmospheric Research*, 247, 105238. <https://doi.org/10.1016/j.atmosres.2020.105238>
- Arevalo, L., & Cooray, V. (2017). Unstable leader inception criteria of atmospheric discharges. *Atmosphere*, 8(9), 156. <https://doi.org/10.3390/atmos8090156>
- Bazelyan, E. M., & Raizer, Y. P. (2000). *Lightning physics and lightning protection*. IOP Publishing.
- Bazelyan, E. M., Raizer, Y. P., & Aleksandrov, N. L. (2007). The effect of reduced air density on streamer-to-leader transition and on properties of long positive leader. *Journal of Physics D*, 40(14), 4133–4144. <https://doi.org/10.1088/0022-3727/40/14/007>
- Biagi, C. J., Uman, M. A., Hill, J. D., Jordan, D. M., Rakov, V. A., & Dwyer, J. (2010). Observations of stepping mechanisms in a rocket-and-wire triggered lightning flash. *Journal of Geophysical Research*, 115, D23215. <https://doi.org/10.1029/2010JD014616>
- Chanrion, O., Neubert, T., Lundgaard Rasmussen, I., Stoltze, C., Tcherniak, D., Jessen, N. C., et al. (2019). The modular multispectral imaging array (MMLA) of the ASIM Payload on the International Space Station. *Space Science Reviews*, 215, 28. <https://doi.org/10.1007/s11214-019-0593-y>

## Acknowledgments

This work has received funding from the European Union Horizon 2020 Framework Program under the Marie Skłodowska-Curie Grant Agreement SAINT 722337. This work was also supported by research Grant ESP2017-86263-C4-2-R funded by MCIN/AEI/10.13039/501100011033 and by “ERDF A way of making Europe”, by the “European Union”; and Grants PIDP2019-109269RB-C42 and ENE2017-91636-EXP funded by MCIN/AEI/10.13039/501100011033.

- Chern, J. L., Hsu, R. R., Su, H. T., Mende, S. B., Fukunishi, H., Takahashi, Y., & Lee, L. C. (2003). Global survey of upper atmospheric transient luminous events on the ROCSAT-2 satellite. *Journal of Atmospheric and Solar-Terrestrial Physics*, 65, 647–659. [https://doi.org/10.1016/S1364-6826\(02\)00317-6](https://doi.org/10.1016/S1364-6826(02)00317-6)
- Christian, H. J., Blakeslee, R. J., & Goodman, S. J. (1989). The detection of lightning from geostationary orbit. *Journal of Geophysical Research*, 94, 13329–13337. <https://doi.org/10.1029/JD094iD11p13329>
- Cooray, V., Cooray, G., Rubinstein, M., & Rachidi, F. (2020). Modeling compact intracloud discharge (CID) as a streamer burst. *Atmosphere*, 11(5), 549–398. <https://doi.org/10.3390/atmos11050549>
- Gallimberti, I. (1979). The mechanism of the long spark formation. *Journal de Physique Colloques*, 40(C7), 193–193. <https://doi.org/10.1051/jphyscol:19797440>
- Gallimberti, I., Bacchiega, G., Bondiou-Clergerie, A., & Lalande, P. (2002). Fundamental processes in long air gap discharges. *Comptes Rendus Physique*, 3(10), 1335–1359. [https://doi.org/10.1016/S1631-0705\(02\)01414-7](https://doi.org/10.1016/S1631-0705(02)01414-7)
- Gallimberti, I., Hepworth, J. K., & Klewe, R. C. (1974). Spectroscopic investigation of impulse corona discharges. *Journal of Physics D*, 7(6), 880–898. <https://doi.org/10.1088/0022-3727/7/6/315>
- Goodman, S. J., Blakeslee, R. J., Koshak, W. J., Mach, D., Bailey, J., Buechler, D., et al. (2013). The GOES-R geostationary lightning mapper (GLM). *Atmospheric Research*, 125, 34–49. <https://doi.org/10.1016/j.atmosres.2013.01.006>
- Heumesser, M., Chanrion, O., Neubert, T., Christian, H. J., Dimitriadou, K., Gordillo-Vázquez, F. J., et al. (2021). Spectral observations of optical emissions associated with terrestrial gamma-ray flashes. *Geophysical Research Letters*, 48, e2020GL090700. <https://doi.org/10.1029/2020GL090700>
- Janda, M., & Machala, Z. (2011). Imaging of transient spark in atmospheric air by Fast iCCD camera. *IEEE Transactions on Plasma Science*, 39(11), 2246–2247. <https://doi.org/10.1109/TPS.2011.2157175>
- Janda, M., Machala, Z., Niklová, A., & Martišovič, V. (2012). The streamer-to-spark transition in a transient spark: A dc-driven nanosecond-pulsed discharge in atmospheric air. *Plasma Sources Science and Technology*, 21(4), 045006. <https://doi.org/10.1088/0963-0252/21/4/045006>
- Janda, M., Martišovič, V., Hensel, K., & Machala, Z. (2016). Generation of antimicrobial NO<sub>x</sub> by atmospheric air transient spark discharge. *Plasma Chemistry and Plasma Processing*, 36, 767–781. <https://doi.org/10.1007/s11090-016-9694-5>
- Jiang, R., Qie, X., Li, Z., Zhang, H., Li, X., Yuan, S., et al. (2020). Luminous crown residual vs. bright space segment: Characteristic structures for the intermittent positive and negative leaders of triggered lightning. *Geophysical Research Letters*, 47(21), e2020GL088107. <https://doi.org/10.1029/2020GL088107>
- Kieu, N., Gordillo-Vázquez, F. J., Passas, M., Sánchez, J., & Pérez-Invernón, F. J. (2021). High-speed spectroscopy of lightning-like discharges: Evidence of molecular optical emissions. *Journal of Geophysical Research: Atmosphere*, 126, e2021JD035016. <https://doi.org/10.1029/2021JD035016>
- Kirkland, M. W., Suszcynsky, D. M., Guillen, J. L. L., & Green, J. L. (2001). Optical observations of terrestrial lightning by the FORTE satellite photodiode detector. *Journal of Geophysical Research*, 106(D24), 33499–33509. <https://doi.org/10.1029/2000JD000190>
- Kochkin, P., Lehtinen, N., van Deursen, A. P. J., & Østgaard, N. (2016). Pilot system development in metre-scale laboratory discharge. *Journal of Physics D*, 49, 425203. <https://doi.org/10.1088/0022-3727/49/42/425203>
- Kochkin, P. O., van Deursen, A. P. J., & Ebert, U. (2014). Experimental study of the spatio-temporal development of metre-scale negative discharge in air. *Journal of Physics D*, 47(14), 145203. <https://doi.org/10.1088/0022-3727/47/14/145203>
- Les Renardières Group. (1981). Negative discharges in long air gaps at Les Renardières—1978 results and conclusions. *Electra*, 74, 67–216.
- Li, D., Luque, A., Gordillo-Vázquez, F. J., Liu, F., Lu, G., Neubert, T., et al. (2021). Blue flashes as counterparts to narrow bipolar events: The optical signal of shallow in-cloud discharges. *Journal of Geophysical Research: Atmosphere*, 126, e2021JD035013. <https://doi.org/10.1029/2021JD035013>
- Montanyà, J., López, J. A., Morales Rodríguez, C. A., van der Velde, O. A., Fabró, F., Pineda, N., et al. (2021). A simultaneous observation of lightning by ASIM, Colombia-lightning mapping array, GLM, and ISS-LIS. *Journal of Geophysical Research: Atmosphere*, 126, e2020JD033735. <https://doi.org/10.1029/2020JD033735>
- Neubert, T., Chanrion, O., Heumesser, M., Dimitriadou, K., Husbjerg, L., Rasmussen, I. L., et al. (2021). Observation of the onset of a blue jet into the stratosphere. *Nature*, 589, 371–375. <https://doi.org/10.1038/s41586-020-03122-6>
- Neubert, T., Østgaard, N., Reglero, V., Blanc, E., Chanrion, O., Oxborrow, C. A., et al. (2019). The ASIM mission on the International Space Station. *Space Science Reviews*, 215, 26. <https://doi.org/10.1007/s11214-019-0592-z>
- Neubert, T., Rycroft, M., Farges, T., Blanc, E., Chanrion, O., Arnone, E., et al. (2008). Recent Results from Studies of Electric Discharges in the Mesosphere. *Surveys in Geophysics*, 29, 71–137. <https://doi.org/10.1007/s10712-008-9043-1>
- Nijdam, S., Teunissen, J., & Ebert, U. (2020). The physics of streamer discharge phenomena. *Plasma Sources Science and Technology*, 29, 103001. <https://doi.org/10.1088/1361-6595/abaa05>
- Østgaard, N., Neubert, T., Reglero, V., Ullaland, K., Yang, S., Genov, G., et al. (2019). First 10 months of TGF observations by ASIM. *Journal of Geophysical Research: Atmosphere*, 124, 14024–14036. <https://doi.org/10.1029/2019JD031214>
- Rakov, V. A., & Uman, M. A. (2003). *Lightning: Physics and effects*. Cambridge University Press.
- Reess, T., Ortega, P., Gibert, P., Domens, P., & Pignolet, P. (1995). An experimental study of negative discharge in a 1.3 m point-plane air gap: The function of the space stem in the propagation mechanism. *Journal of Physics D*, 28, 2306. <https://doi.org/10.1088/0022-3727/28/11/011>
- Rison, W., Krehbiel, P., Stock, M., Edens, H. E., Shao, X.-M., Thomas, R. J., et al. (2016). Observations of narrow bipolar events reveal how lightning is initiated in thunderstorms. *Nature Communications*, 7, 10721. <https://doi.org/10.1038/ncomms10721>
- Saba, M. M. F., de Paiva, A. R., Concolato, L. C., Warner, T. A., & Schumann, C. (2020). Optical observation of needles in upward lightning flashes. *Scientific Reports*, 10, 17460. <https://doi.org/10.1038/s41598-020-74597-6>
- Soler, S., Perez-Invernón, F. J., Gordillo-Vázquez, F. J., Luque, A., Li, D., Malagón-Romero, A., et al. (2020). Blue optical observations of narrow bipolar events by ASIM suggest corona streamer activity in thunderstorms. *Journal of Geophysical Research: Atmosphere*, 125, e2020JD032708. <https://doi.org/10.1029/2020JD032708>
- van der Velde, O., Montanyà, J., Neubert, T., Chanrion, O., Lopez, J. A., Fabró, F., et al. (2020). Comparison of high-speed optical observations of a lightning flash from space and the ground. *Earth and Space Science*, 7, e2020EA001249. <https://doi.org/10.1029/2020EA001249>
- Wu, C., Xie, S., Qi, F., Li, B., Wan, J., & He, J. (2013). Effect of corona discharges on the inception of positive upward leader-streamer system. *International Journal of Modern Physics B*, 27, 1350165. <https://doi.org/10.1142/S0217979213501658>
- Zhao, X., Becerra, M., Yang, Y., & He, J. (2021). Elongation and branching of stem channels produced by positive streamers in long air gaps. *Scientific Reports*, 11, 4120. <https://doi.org/10.1038/s41598-021-83816-7>
- Zhao, X., Liu, X., Yang, Y., Wang, X., Liu, Y., & He, J. (2021). Observations of the channel illuminations during dark periods in long positive sparks. *Geophysical Research Letters*, 48, e2020GL091815. <https://doi.org/10.1029/2020GL091815>